

**“Click-chemistry” approach in the design of 1,2,3-triazolyl-pyridine ligands and their Ru(II)-complexes for dye-sensitized solar cells**Ilona Stengel,<sup>a</sup> Amaresh Mishra,<sup>a</sup> Nuttapol Pootrakulchote,<sup>b</sup> Soo-Jin Moon,<sup>b</sup> Shaik M. Zakeeruddin,<sup>\*b</sup> Michael Grätzel<sup>\*b</sup> and Peter Bäuerle<sup>\*a</sup>

Received 2nd November 2010, Accepted 13th December 2010

DOI: 10.1039/c0jm03750h

The synthesis of new 1,2,3-triazolyl-pyridine ligands *via* “click-chemistry” and their corresponding Ru(L)(2,2'-bipyridyl-4,4'-dicarboxylic acid)(NCS)<sub>2</sub> complexes (L = 1,2,3-triazolyl-pyridine) are presented. The complexes have been photophysically and electrochemically characterized and have been used as sensitizers in dye-sensitized solar cells (DSSC). In DSSCs with an acetonitrile-based electrolyte the cells comprising of Ru(2-(1-(4-hexylphenyl)-1*H*-1,2,3-triazol-4-yl)pyridine)(2,2'-bipyridyl-4,4'-dicarboxylic acid)(NCS)<sub>2</sub> TBA salt **1** showed an overall power conversion efficiency of 7.8% under full sunlight intensity, and Ru(2-(4-(4-hexylphenyl)-1*H*-1,2,3-triazol-1-yl)pyridine)(2,2'-bipyridyl-4,4'-dicarboxylic acid)(NCS)<sub>2</sub> TBA salt **2** an efficiency of 4.7%. Transient photovoltage and photocurrent decay measurements showed an enhanced performance for dye **1** due to faster electron transport into the TiO<sub>2</sub> film and lower recombination rate in comparison to dye **2** sensitized devices. Additionally, solid-state devices were prepared with 2 μm thick TiO<sub>2</sub> films using spiro-OMeTAD as a hole-transport material. The solid-state dye-sensitized solar cells showed power conversion efficiencies of 1.92% and 0.38% for sensitizer **1** and **2**, respectively.

**Introduction**

Dye-sensitized solar cells (DSSC) have attracted great interest in materials science in the past years. First results were reported in 1991,<sup>1</sup> and ever since chemists are in search of new dyes which appear as suitable sensitizers in titanium dioxide-based organic photovoltaic cells.<sup>2</sup> DSSCs with power conversion efficiencies over 10% were initially demonstrated using prototype *cis*-di(thiocyanato)-*bis*[2,2'-bipyridyl-4,4'-dicarboxylic acid] Ru(II) (N3), its *bis*-tetrabutylammonium (TBA) salt counterpart N719 or black dye [tri(thiocyanato)-(4,4',4''-[2,2':6',2''-terpyridine] tricarboxylic acid) Ru(II) as sensitizers. The dyes are the key-components in DSSCs as they absorb sunlight and induce intramolecular charge transfer from the ancillary ligand to the anchoring ligand with subsequent electron injection into the TiO<sub>2</sub> semiconductor. In this respect, numerous reports about bipyridine-Ru(II) dyes, which, for example were functionalized with either hydrophobic chains to improve the device stability or with elongated π-systems to enhance absorption have been published.<sup>3</sup>

In general, bi- and terpyridines (*bpy* and *terpy*) are the most frequently investigated ligands for ruthenium(II) complexes.<sup>4</sup> Relatively little is known about Ru(II) complexes in which 1,2,4-triazoles<sup>5</sup> or 1,2,3-triazoles are used as chelating ligands. However, growing interest in 1,2,3-triazolyl-derivatives as chelates is evolving since 2001, when the “click-chemistry” approach was presented.<sup>6a</sup> In particular, the 1,3-dipolar Cu(I)-catalyzed Huisgen cycloaddition of azides and terminal acetylenes is widely used in various areas in order to build up a diverse series of 1,2,3-triazoles under mild reaction conditions and in high yields.<sup>6-8</sup>

Very recently, several bi- and terdentate ligands such as (1,2,3-triazol-4-yl)pyridines,<sup>7a,c,d,8a,b</sup> 2,6-bis(1,2,3-triazol-4-yl)pyridines<sup>7b,8c</sup> and 4,4'-bis(1,2,3-triazoles)<sup>7c-e</sup> and their corresponding Ru(II) complexes were synthesized using click-chemistry. Crystallographic analysis has shown that upon replacing one pyridyl unit with one triazolyl unit in the Ru(II) coordination sphere, the geometry of the complex is only slightly affected.<sup>8b,c</sup> Complexes with asymmetrical triazolyl-pyridine ligands were generally isolated as isomeric mixtures. Concerning the photophysical properties of such compounds, it was observed that with an increasing number of triazole rings the HOMO/LUMO energy gap of the octahedral Ru(II) complex increases in comparison to their bi- and terpyridine counterparts.<sup>8a,c</sup> As a result, the absorption and emission spectra are blue-shifted. Triazolyl-pyridine has a higher acceptor strength compared to bipyridine, therefore, better back-bonding from the Ru(II) metal centre to the ligand-centered π\* orbital is possible, which lowers the metal-centered highest

<sup>a</sup>Institute of Organic Chemistry II and Advanced Materials, University of Ulm, Albert-Einstein-Allee 11, D-89081 Ulm, Germany. E-mail: peter.baeuerle@uni-ulm.de; Fax: +49 (0)731 50 22840

<sup>b</sup>Laboratory for Photonics and Interfaces, Institute of Chemical Sciences and Engineering, School of Basic Sciences, Swiss Federal Institute of Technology, CH-1015 Lausanne, Switzerland. E-mail: shaik.zakeer@epfl.ch; michael.graetzel@epfl.ch; Fax: +41 (0)21 693 61 00

occupied molecular orbital (HOMO) and increases the  $\pi^*$  orbital energy of the triazolyl ligand. In heteroleptic complexes, with one *bpy* ligand and a triazolyl-pyridine ligand, the lowest unoccupied molecular orbital (LUMO) is mostly located on the *bpy* ligand, because the  $\pi^*$  orbital of the triazole ligand is more destabilized. In general, one can say that the LUMO is shifted to higher energies with an increasing number of triazole units in the Ru(II) complex, but it also strongly depends on the nature of the substituents which are attached to the triazole or the pyridine. Acceptor substituents are able to lower the LUMO energy and they show the biggest influence if they are linked to the *bpy* chelator or to the pyridine moiety in the triazolyl-pyridine ligand.<sup>8</sup>

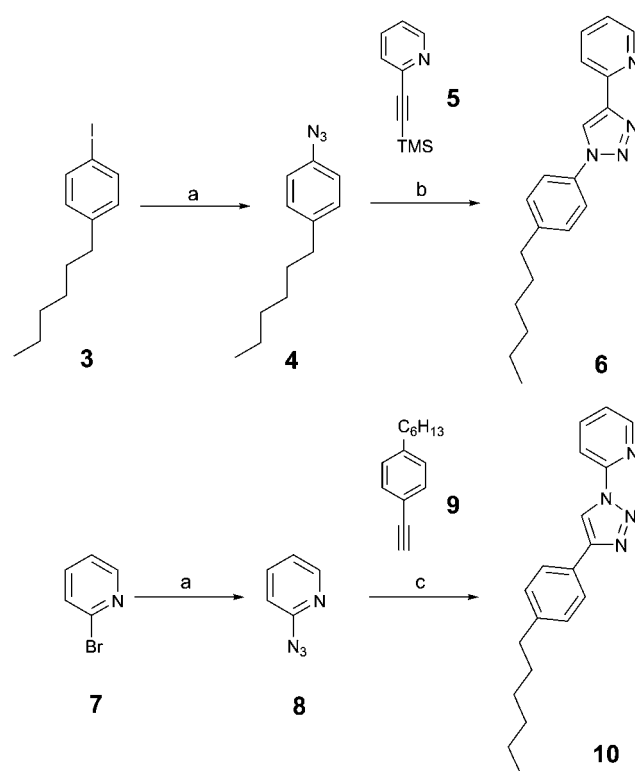
In search of new ligands for Ru(II) dyes in DSSCs it is shown that pyridines can successfully be replaced by other N-containing ligands, for example, pyrazoles.<sup>9</sup> In a recent report, the click-chemistry approach was used to functionalize the periphery of an ancillary bipyridine-ligand in a Ru(II) dye,<sup>10</sup> while there are no examples reported up to now where 1,2,3-triazoles have been used as chelating ligands in Ru(II) sensitizers for solar cell applications. In order to gain more insight into structure–property–device performance relationships, we report herein the synthesis of new dithiocyanato-(1*H*-1,2,3-triazolyl-pyridine)(2,2'-bipyridyl-4,4'-carboxylic acid) ruthenium(II) dyes **1** and **2**. The photophysical and electrochemical investigations provide insight into the electronic structure and potential applicability of the novel dyes. The complexes were incorporated and characterized in DSSCs using a volatile solvent-based electrolyte on one hand and a solid-state organic hole conductor (spiro-MeOTAD) as redox mediator on the other hand.

## Results and discussion

### Synthesis

Azides **4** and **8** were synthesized from their corresponding halides *via* a Cu(I)-catalyzed substitution reaction with sodium azide,<sup>11</sup> (Scheme 1). The click-reaction was performed either by *in situ* deprotection of the trimethylsilyl-protected ethynyl group with potassium fluoride or directly with the deprotected ethynyl compound. Ligand **6** was obtained in 89% yield by the Cu(I)-catalyzed click-reaction of azide **4** and trimethylsilyl-protected ethynylpyridine **5** at room temperature. However, in the case of ligand **10** the reaction is much slower at room temperature. Therefore, click-reaction of azide **8** and ethynyl compound **9** were performed under reflux conditions for five days and ligand **10** was obtained in 73% yield.

The Ru(II) dyes **1** and **2** were obtained from a one-pot synthesis in which di- $\mu$ -chloro(*p*-cymene)ruthenium(II) dimer was used as a precursor (Scheme 2). In a first step, the Ru(II) precursor was reacted with ligands **6** and **10**, respectively, in the second step, 2,2'-bipyridyl-4,4'-dicarboxylic acid (dcbpy) was introduced and in the last reaction step thiocyanate was added. Both complexes were purified *via* Sephadex LH-20 column chromatography with methanol as eluent. After precipitation, the dyes were isolated as mono-TBA salt. The structures were confirmed by <sup>1</sup>H-NMR and ESI high resolution mass spectroscopy. The proton NMR spectrum showed two isomers for each compound (*fac*- and *mer*-isomer in a ratio of 2 : 1 for **1** and 3 : 1 for **2**), which could not be



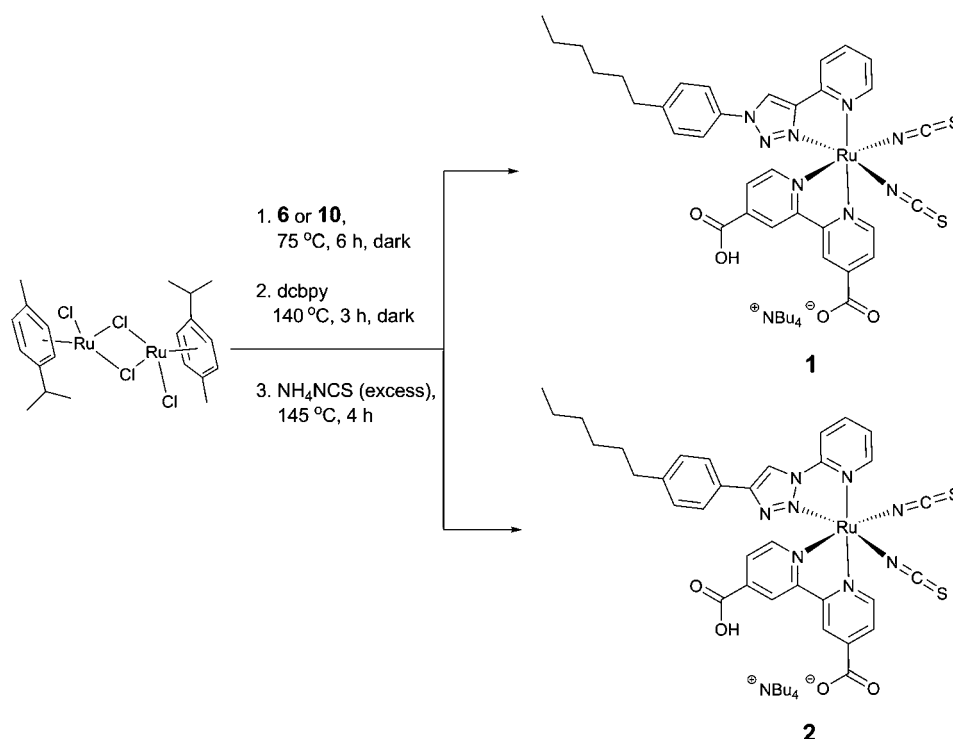
**Scheme 1** Synthesis of bidentate 1,2,3-triazolyl-pyridine ligands. a)  $\text{NaN}_3$ , CuI, Na ascorbate, DMEDA, EtOH–water (7 : 3), 100 °C, 1 h, 92% (**4**) and 68% (**8**). b) KF,  $\text{Cu}(\text{CH}_3\text{CN})_4\text{PF}_6$ ,  $\text{Cu}^0$ , DIPEA, DCM–MeOH (4 : 1), rt, 3 d, 89%. c)  $\text{Cu}(\text{CH}_3\text{CN})_4\text{PF}_6$ ,  $\text{Cu}^0$ , DIPEA, DCM–MeOH (4 : 1), reflux, 5 d, 73%.

separated *via* column chromatography. It has been previously reported that the isomers are generally difficult to separate when bidentate triazolyl-pyridine were used as ligands.<sup>8a</sup>

### Photophysical properties

Absorption and emission spectra of dyes **1** and **2** are depicted in Fig. 1. Both dyes show broad absorption from the UV region up to 650 nm. The high energy absorption band at 250–300 nm can be assigned to intraligand  $\pi$ – $\pi^*$  transitions. Both dyes show two additional absorption bands at lower energies which can be attributed to metal-to-ligand charge transfer transitions (MLCT). Dye **1** showed the lowest energy MLCT absorption band at 493 nm with a molar extinction coefficient of 7600  $\text{L mol}^{-1} \text{cm}^{-1}$ , which is lower than the higher energy MLCT band ( $\lambda_{\text{max}} = 369 \text{ nm}$ ,  $\epsilon = 12000 \text{ L mol}^{-1} \text{cm}^{-1}$ ). In contrast, dye **2** showed the lowest energy MLCT band at 465 nm with a higher extinction coefficient of 9200  $\text{L mol}^{-1} \text{cm}^{-1}$  than the higher energy MLCT band at 366 nm ( $\epsilon = 8000 \text{ L mol}^{-1} \text{cm}^{-1}$ ). The lowest energy MLCT band of **2** is blue-shifted by 30 nm compared to **1**. In comparison to bipyridine-based Ru(II) dyes the new dyes exhibit blue-shifted absorption bands with lower molar extinction coefficients.<sup>3</sup>

Emission maxima of dyes **1** and **2** are found at 738 and 765 nm, respectively, when excited at 480 nm, in the region of the lowest energy MLCT absorption. A large Stoke's shift was observed for both dyes **1** ( $6734 \text{ cm}^{-1}$ ) and **2** ( $8433 \text{ cm}^{-1}$ ), which is an indication of significant structural changes between the ground and excited



Scheme 2 Synthesis of Ru(II) dyes 1 and 2.

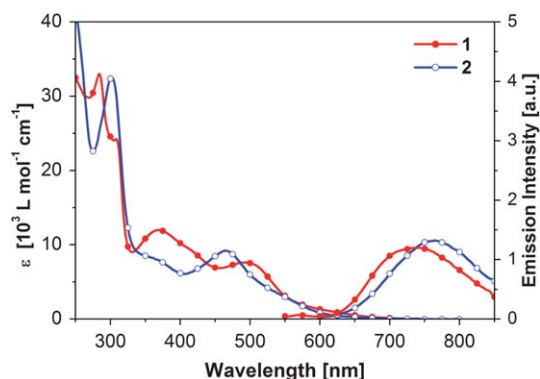


Fig. 1 UV-VIS and normalized emission spectra of dye 1 and 2, measured in acetonitrile. Emission spectra were measured in aerated acetonitrile solution with  $c \sim 10^{-5} \text{ mol L}^{-1}$  ( $\lambda_{\text{ex}} = 480 \text{ nm}$ ).

state. Similar to the absorption spectra, the emission bands are also blue-shifted compared to bipyridine-based Ru(II)-complexes.

### Electrochemical properties

The redox behaviour of the dyes was measured by cyclic voltammetry (CV) and differential pulse voltammetry (DPV) in DMF solutions containing 0.1 M tetrabutylammonium hexafluorophosphate (TBAPF<sub>6</sub>) as the supporting electrolyte (Fig. 2). The data is presented in Table 1. The redox properties of both dyes are similar. They show two irreversible oxidation waves, one around 0.3 V and the second at about 0.4 V vs. Fc/Fc<sup>+</sup>. The first oxidation wave can be attributed to the Ru<sup>II</sup>/Ru<sup>III</sup> oxidation, whereas the second wave can be assigned to the oxidation of the

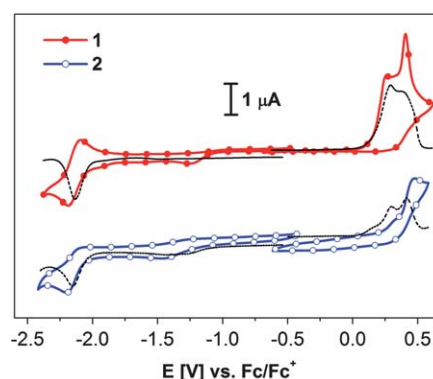


Fig. 2 Cyclic voltammogram (CV) of dye 1 and 2, in DMF (0.1 M TBAPF<sub>6</sub>),  $c = 10^{-3} \text{ mol L}^{-1}$ . The differential pulse voltammogram (DPV) plots are presented as black dashed lines.

NCS ligand. Both dyes 1 and 2, display one reversible reduction wave at  $-2.15 \text{ V}$ , which can be assigned to the one electron reduction of the *dcbpy* ligand. The HOMO/LUMO energy levels were calculated from the onset of the first oxidation and reduction waves, respectively. The smaller band gap obtained for 1 ( $E_g = 2.12 \text{ eV}$ ) compared to 2 ( $E_g = 2.19 \text{ eV}$ ) is in agreement with the red-shift of the absorption spectrum. For an efficient sensitizer in DSSCs the LUMO energy level has to be higher in energy than the quasi-Fermi level of the TiO<sub>2</sub> photoanode, ensuring efficient electron transfer from the excited dye into the titanium dioxide semiconductor. The HOMO level has to be sufficiently low in energy to accept electrons from the I<sub>3</sub><sup>-</sup>/I<sup>-</sup>-based redox electrolyte (Fig. 3). Thus, the HOMO/LUMO energy values of 1 and 2 fit well with the energy levels of TiO<sub>2</sub> ( $-4.0 \text{ eV}$  vs. vacuum) and I<sub>3</sub><sup>-</sup>/I<sup>-</sup> ( $-4.83 \text{ eV}$  vs. vacuum).

**Table 1** Photophysical and electrochemical data of complexes **1** and **2**

Dye	$\lambda_{\text{abs}}$ [nm] <sup>a</sup> ( $\epsilon$ [L mol <sup>-1</sup> cm <sup>-1</sup> ])	$\lambda_{\text{em}}$ [nm] <sup>a</sup>	$E_{\text{ox1}}^0$ [V] <sup>b</sup>	$E_{\text{ox2}}^0$ [V] <sup>b</sup>	$E_{\text{red}}^0$ [V] <sup>b</sup>	HOMO [eV] <sup>c</sup>	LUMO [eV] <sup>c</sup>	$E_g$ [eV] <sup>d</sup>
<b>1</b>	284 (33 000)	738	0.29	0.37	-2.14	-5.23	-3.11	2.12
	369 (12 000)							
	493 (7600)							
<b>2</b>	302 (32500)	765	0.32	0.42	-2.15	-5.28	-3.09	2.19
	366 (8 000)							
	465 (9200)							

<sup>a</sup> Measured in acetonitrile solution. <sup>b</sup> Measured vs. Fc/Fc<sup>+</sup> in DMF (0.1 M TBAPF<sub>6</sub>), [c] =  $\sim 10^{-3}$  mol L<sup>-1</sup>, 295 K, scan rate = 100 mV s<sup>-1</sup>. Potentials were determined using DPV. <sup>c</sup> Determined from the onsets of oxidation and reduction waves, set Fc<sup>+</sup>/Fc  $E_{\text{HOMO}} = -5.1$  eV.<sup>12</sup> <sup>d</sup> Calculated by the difference of the values of  $E_{\text{red1 onset}}$  and  $E_{\text{ox1 onset}}$ .

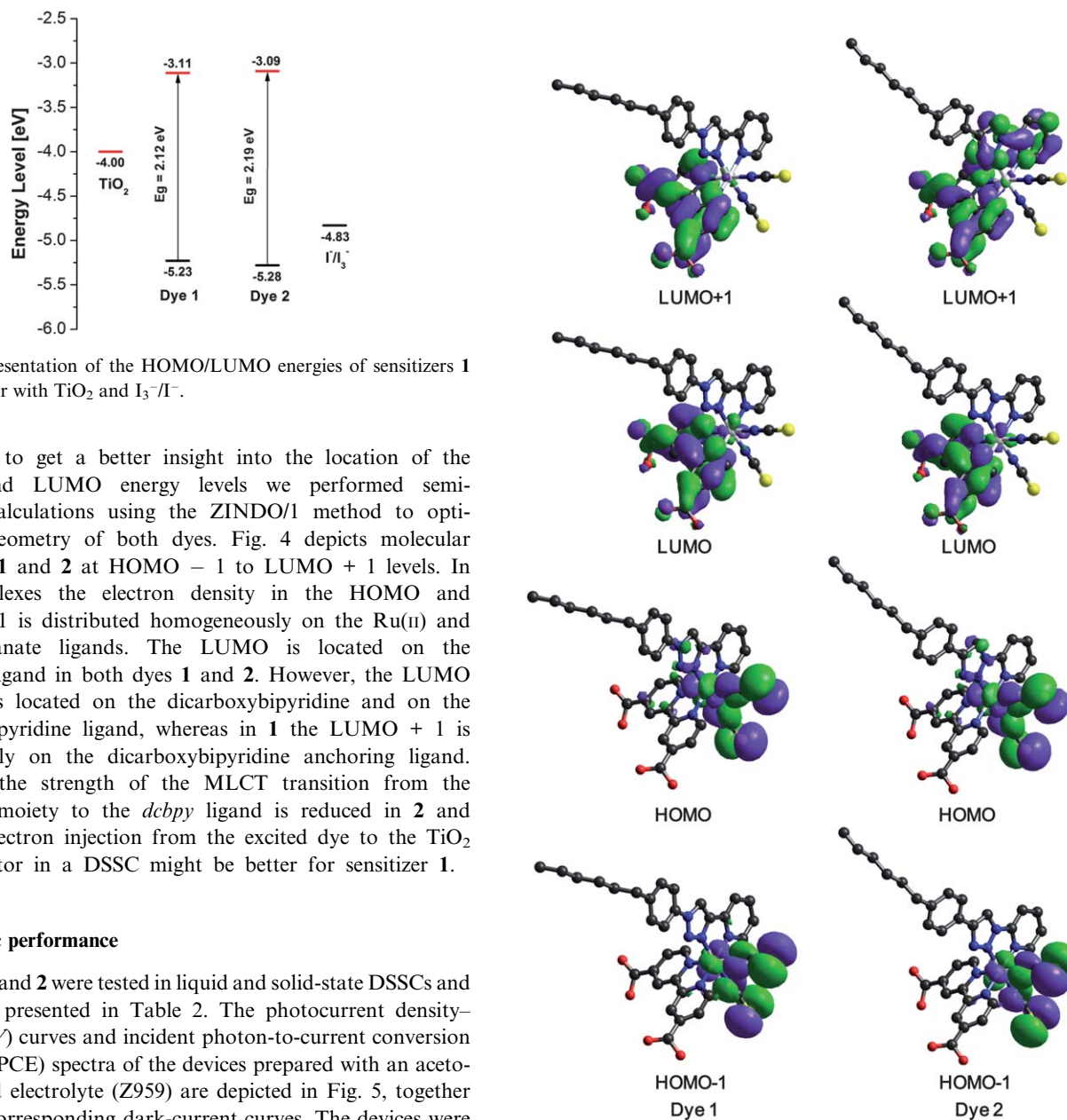


**Fig. 3** Representation of the HOMO/LUMO energies of sensitizers **1** and **2** together with TiO<sub>2</sub> and I<sub>3</sub><sup>-</sup>/I<sup>-</sup>.

In order to get a better insight into the location of the HOMO and LUMO energy levels we performed semi-empirical calculations using the ZINDO/1 method to optimize the geometry of both dyes. Fig. 4 depicts molecular orbitals of **1** and **2** at HOMO - 1 to LUMO + 1 levels. In both complexes the electron density in the HOMO and HOMO - 1 is distributed homogeneously on the Ru(II) and the thiocyanate ligands. The LUMO is located on the anchoring ligand in both dyes **1** and **2**. However, the LUMO + 1 in **2** is located on the dicarboxybipyridine and on the triazol-1-yl-pyridine ligand, whereas in **1** the LUMO + 1 is situated only on the dicarboxybipyridine anchoring ligand. Therefore, the strength of the MLCT transition from the Ru(NCS)<sub>2</sub> moiety to the *dcbpy* ligand is reduced in **2** and therefore electron injection from the excited dye to the TiO<sub>2</sub> semiconductor in a DSSC might be better for sensitizer **1**.

### Photovoltaic performance

Both dyes **1** and **2** were tested in liquid and solid-state DSSCs and the data is presented in Table 2. The photocurrent density–voltage (*J*–*V*) curves and incident photon-to-current conversion efficiency (IPCE) spectra of the devices prepared with an acetonitrile-based electrolyte (Z959) are depicted in Fig. 5, together with their corresponding dark-current curves. The devices were prepared using a double layer TiO<sub>2</sub> film which consisted of a transparent 8 μm thick layer and a 5 μm scattering layer, and DINHOP (dineohexyl bis(3,3-dimethylbutyl)phosphinic acid) was added as co-adsorbent to the dye solution. The IPCE

**Fig. 4** Graphical representation of the frontier orbitals of **1** and **2** optimized using the ZINDO/1 semi-empirical method. Atoms: C black, N blue, S yellow, O red, Ru brown.

**Table 2** Summarized data of the liquid and solid-state DSSC performance

Dye	Device	$V_{OC}$ [mV]	$J_{SC}$ [ $\text{mA cm}^{-2}$ ]	$FF$	$\eta$ [%]	IPCE <sub>max</sub> [%] ( $\lambda$ [nm])
1	liquid <sup>a</sup>	761	13.2	0.77	7.8	77(500)
2	liquid <sup>a</sup>	673	8.9	0.77	4.7	58 (480)
1	solid <sup>b</sup>	692	4.05	0.68	1.92	33 (500)
2	solid <sup>b</sup>	569	0.98	0.69	0.38	8 (460)

<sup>a</sup> Liquid device: Electrolyte: Z959; co-adsorbent: DINHOP (4 : 1); film thickness: 8 + 5  $\mu\text{m}$ . <sup>b</sup> Solid-state device: Spiro-OMeTAD as hole conductor, *tert*-Butyl pyridine and  $\text{Li}(\text{CF}_3\text{SO}_2)_2\text{N}$ .

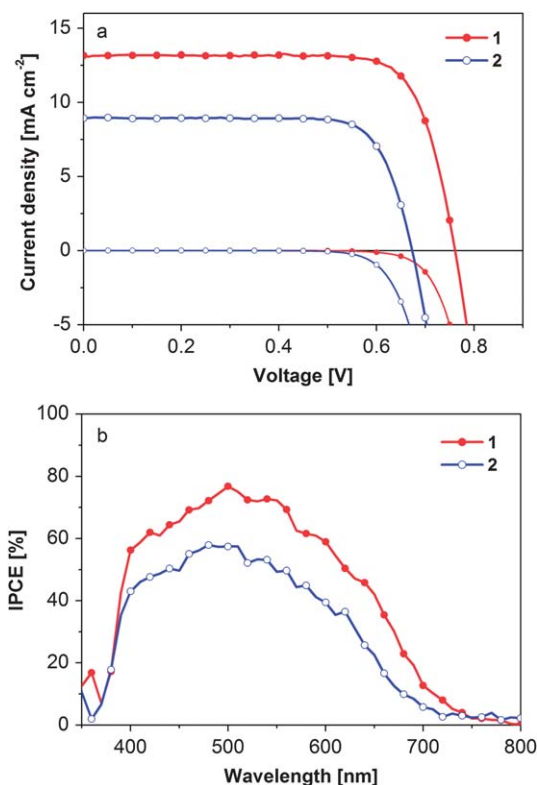


**Fig. 5** (a) Photocurrent density–Voltage ( $J$ – $V$ ) characteristic and (b) incident photon-to-current conversion efficiency (IPCE) spectrum of acetonitrile-based devices using **1** and **2** sensitizers. Electrolyte composition (Z959): 1.0 M 1,3-dimethylimidazolium iodide, 0.03 M iodine, 0.1 M guanidinium thiocyanate, 0.5 M *tert*-butylpyridine in acetonitrile/valeronitrile (85 : 15).

spectrum of **1** covers a broad range from 380 to 700 nm, reaching its maximum of 77% at 500 nm, whereas the IPCE spectrum of **2** is slightly blue-shifted with a maximum of 58% at 480 nm.

Under full sunlight (AM 1.5 G,  $100 \text{ mW cm}^{-2}$ ) the dye **1**-sensitized device exhibited an open-circuit photovoltage ( $V_{OC}$ ), a short-circuit photocurrent density ( $J_{SC}$ ), fill-factor ( $FF$ ) and power conversion efficiency ( $\eta$ ) of 761 mV,  $13.2 \text{ mA cm}^{-2}$ , 0.77 and 7.8%, respectively. On the other hand, a dye **2**-sensitized device gave a  $V_{OC}$  of 673 mV,  $J_{SC}$  of  $8.9 \text{ mA cm}^{-2}$ , and  $FF$  of 0.77, yielding a lower  $\eta$  of 4.7%. The power conversion efficiency of dye **1** bearing the 1,2,3-triazol-4-yl ligand is superior to the 1,2,3-triazol-1-yl counterpart dye **2** under similar conditions. Considering the lower molar extinction coefficient and the blue-shift in the absorption spectrum of **1** compared to other bipyridine-based Ru(II) sensitizers, such as Z-907,<sup>3c</sup> the device with

a power conversion efficiency of 7.8% is quite impressive. The higher photocurrent density in the case of the dye **1**-based device can be explained by an increase in the light absorbing capability of the dye **1**-sensitized  $\text{TiO}_2$  film. The higher  $V_{OC}$  in case of the dye **1**-based device is due to either the reduction of charge recombination or the upward shift of the conduction-band edge position. In order to elaborate more on this assumption, transient absorption spectroscopy (TAS) measurements were performed on these devices.

As shown in Fig. 6a, the structural differences of the two sensitizers have a significant effect on the photocurrent decay rate across the  $\text{TiO}_2$  film and on the slope of decay rate vs. charge density measured under open circuit conditions. At identical charge density, the photoinduced electrons in the case of the dye **1**-based device diffuse faster through the  $\text{TiO}_2$  film than those of

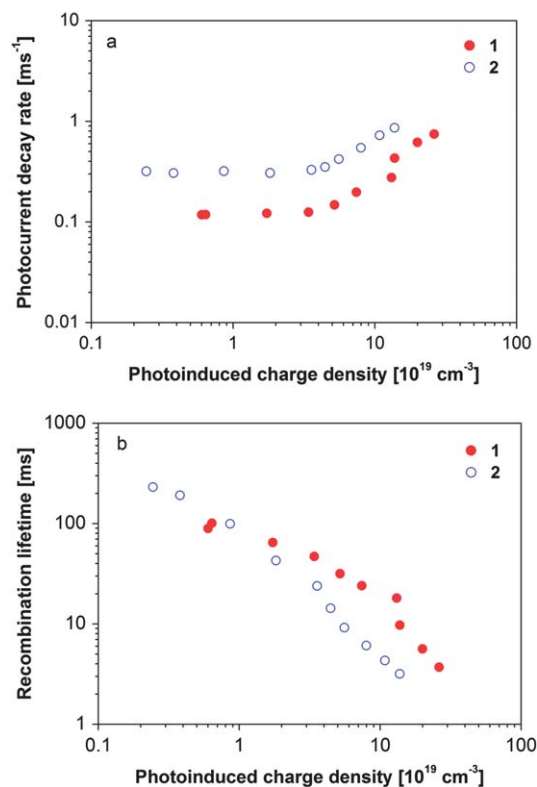


**Fig. 6** (a) Open circuit transient photocurrent decay rate for DSSC devices sensitized with complexes **1** and **2** as a function of photoinduced charge density. (b) Charge recombination lifetime vs. photoinduced charge density of the two devices measured at open circuit conditions.

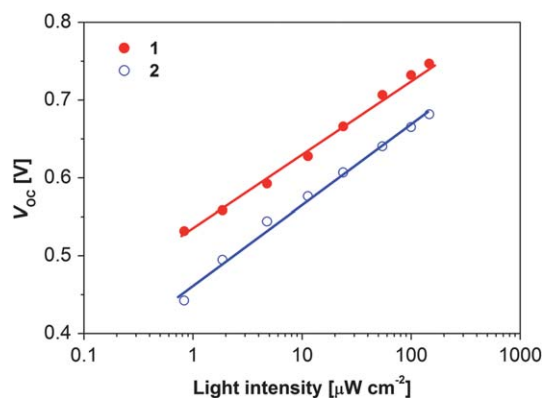


**Fig. 7** Open-circuit voltage of the DSSC based on sensitizer **1** and **2**, plotted *versus* the light intensity, with illumination from a white LED light source.

the dye **2**-based device, resulting from a larger number of occupied trap states for the given Fermi level in the TiO<sub>2</sub> film.

Fig. 6b shows the dependence of the charge recombination lifetime on the photoinduced charge density. The recombination lifetime is determined by the reciprocal of the photovoltage decay rate obtained from a small perturbation voltage decay technique. The value of the charge density is obtained from the experimental measurements by collecting electrons when switching the device from open circuit to short circuit conditions.<sup>13</sup> It is noted that the dye **1**-sensitized device shows a longer charge recombination lifetime than that of the dye **2**-sensitized device at an identical photoinduced charge density, clearly suggesting an advantage of **1** in retarding charge recombination. However, this influence becomes smaller under incident low light intensity where fewer charges are accumulated in the TiO<sub>2</sub> film.

The  $V_{OC}$  as a function of incident light intensity is displayed in Fig. 7. The  $V_{OC}$  of both devices changes linearly according to the logarithm of the light intensity with the slope of 99 mV per decade and 102 mV per decade for devices sensitized with dyes **1** and **2**, respectively. The almost identical slopes indicate that the trap states on the surface of TiO<sub>2</sub> are identical when both dyes are sensitized on TiO<sub>2</sub>. The slope of 59 mV per decade is reported for an ideal diode.<sup>14a</sup> The difference in the slope between the ideal diode and the real devices is attributed to a non-linear recombination occurring in the DSSCs.<sup>14b</sup>

The **1** and **2** dyes were also used as sensitizers for solid-state devices using spiro-OMeTAD (2,2',7,7'-tetrakis(*N,N*-di-*p*-methoxyphenyl-amine)-9,9'-spirobifluorene) as a hole transport material. The power conversion efficiencies of 1.92% and 0.38% were obtained for **1**- and **2**-containing devices, respectively. The corresponding photovoltaic parameters are tabulated in Table 2. Similar to the liquid-devices, in the solid-state cells dye **1** outperforms dye **2** sensitized cells. In comparison to liquid electrolyte devices, the  $J_{SC}$  of the solid-state devices are lower. This is mainly due to thin TiO<sub>2</sub> films (2 μm) used in the solid-state devices which limits the photocurrent density.

## Conclusion

We have shown that click-chemistry is a beneficial approach in the design of new chelating ligands for Ru(II) sensitizers in

DSSCs. Two new substituted 1,2,3-triazole ligands were synthesized *via* the 1,3-dipolar Cu(I)-catalyzed Huisgen cycloaddition (click-reaction). Their corresponding heteroleptic Ru(II) complexes **1** and **2** were prepared and used as sensitizers in liquid and solid-state DSSCs. They have shown overall power conversion efficiencies up to 7.8% which is a remarkable value considering that in comparison to other bipyridine-based Ru(II) sensitizers the absorption spectra are considerably blue-shifted and the molar extinction coefficients are significantly lower. The transient absorption spectral studies revealed that the higher photovoltaic performance of devices with dye **1** is due to the faster electron transport into the TiO<sub>2</sub> film and a lower recombination rate in comparison to the dye **2**-sensitized devices. The large difference in device performance correlates with minor structural changes in the isomeric ligands **4** and **8**, and in the corresponding Ru(II) complexes **1** and **2**, which is the different substitution pattern of the 1,2,3-triazole unit. Taking into account that it is possible to red-shift and to increase the absorption of these dyes by, *e.g.*, extending the  $\pi$  conjugation, a new class of highly efficient 1,2,3-triazolyl-pyridine Ru(II) sensitizers should be accessible *via* the convenient and versatile click-approach.

## Experimental

### Synthesis

1-Iodo-4-*n*-hexylbenzene was purchased from *Alfa Aesar*, sodium azide, copper iodide and Cu(CH<sub>3</sub>CN)<sub>4</sub>PF<sub>6</sub> were purchased from *Aldrich*, sodium ascorbate, 2,2'-bipyridine, 4,4'-dicarboxylic acid (*dc bpy*) and di- $\mu$ -chlorobis[(*p*-cymene)chlororuthenium(II)] ([RuCl<sub>2</sub>(*p*-cymene)]<sub>2</sub>) were purchased from *ABCR*, *N,N'*-dimethylethylenediamine (DMEDA) was purchased from *Acros* and 2-bromopyridine, diisopropylethylamine (DIPEA) and potassium fluoride were purchased from *Merck*. All chemicals were used as received. 2-(TMS-ethynyl)pyridine **5** was synthesized from 2-bromopyridine and trimethylsilylacetylene *via* a Sonogashira coupling reaction according to the literature,<sup>15</sup> and 1-ethynyl-4-*n*-hexylbenzene **9** was synthesized from 1-iodo-4-*n*-hexylbenzene and trimethylsilylacetylene with subsequent deprotection with potassium fluoride (KF) in dichloromethane (DCM) and methanol (MeOH) in the same way.

NMR spectra were recorded on an *Avance 400* spectrometer (<sup>1</sup>H NMR: 400 MHz), at 25 °C. Chemical shift values ( $\delta$ ) are expressed in parts per million using residual solvent protons (CDCl<sub>3</sub>: <sup>1</sup>H  $\delta$  = 7.26 ppm and <sup>13</sup>C  $\delta$  = 77.0 ppm) as internal standard. Chemical shifts of the isomer are given in square brackets. Melting points were determined using a *Buchi B-545* apparatus. Elemental analyses were performed on an *Elementar Vario EL* (University of Ulm). CI mass spectra were recorded on a *Finnigan MAT SSQ-7000*. High resolution mass spectra (HRMS) were measured at the University of Stuttgart with a *micrOTOF-Q43* apparatus and ESI source. Optical measurements were carried out in 1 cm cuvettes with *Merck* spectroscopic grade solvents, absorption spectra were recorded on a *Perkin Elmer Lambda 19* spectrometer and fluorescence spectra on a *Perkin Elmer LS 55* spectrometer. The emission spectra are fully corrected for the photodetector response. IR

spectroscopy was measured on a *Perkin Elmer FT-IR Spectrum 2000*. Cyclic voltammetry experiments were performed with a computer-controlled *Autolab PGSTAT30* potentiostat in a three-electrode single-compartment cell with a platinum working electrode, a platinum wire counter electrode, and an Ag/AgCl reference electrode. All potentials were internally referenced to the ferrocene/ferrocenium (Fc/Fc<sup>+</sup>) couple.

#### 1-Azido-4-n-hexylbenzene (4)

2.0 g (6.94 mmol) 1-Iodo-4-n-hexylbenzene was dissolved in 28 ml ethanol and 12 ml water and the solution was degassed. 0.902 g (13.88 mmol) Sodium azide, 0.131 g (0.69 mmol) CuI, 0.069 g (0.35 mmol) sodium ascorbate and 0.11 ml (1.04 mmol, 0.092 g) DMEDA were added. The suspension was heated under reflux for 45 min. After cooling to room temperature (rt) the reaction mixture was diluted with 100 ml water and extracted with 70 ml diethyl ether three times. The combined organic layers were dried over Na<sub>2</sub>SO<sub>4</sub> and the solvent was removed in vacuo. It was purified *via* column chromatography with silica and petrol ether (PE). The yellow liquid was dried in vacuo and 1.29 g (6.36 mmol, 92%) of the product was obtained. <sup>1</sup>H-NMR (CDCl<sub>3</sub>, 400 MHz): δ = 0.89 (m, 3H, H-6'), 1.30 (m, 6H, H-3', H-4', H-5'), 1.59 (qui, 2H, <sup>3</sup>J = 7.6 Hz, H-2'), 2.59 (t, 2H, <sup>3</sup>J = 7.7 Hz, H-1'), 6.95 (d, 2H, <sup>3</sup>J = 8.4 Hz, H-2), 7.16 (d, 2H, <sup>3</sup>J = 8.4 Hz, H-3). <sup>13</sup>C-NMR (CDCl<sub>3</sub>, 100 MHz): δ = 14.1 (C-6'), 22.6 (C-5'), 28.9, 31.4, 31.7 (C-2', C-3', C-4'), 35.3 (C-1'), 118.8 (C-2), 129.7 (C-3), 137.3 (C-1), 139.8 (C-4). MS (CI, 100 eV): *m/z* = 204 (43%, M + H<sup>+</sup>), 176 (100%), 132 (9%). *R<sub>F</sub>*-value: 0.69 (silica, PE). IR (NaCl): [cm<sup>-1</sup>] = 2106 (s, azide). Elemental analysis (%): calc. C: 70.90, H: 8.43, N: 20.67; found C: 70.79, H: 8.47, N: 20.77.

#### 2-(1-(4-Hexylphenyl)-1H-1,2,3-triazol-4-yl)pyridine (6)

1.0 g (4.92 mmol) 1-Azido-4-n-hexylbenzene **4** and 0.862 g (4.92 mmol) 2-(TMS-ethynyl)pyridine were dissolved in 30 ml DCM and 6 ml methanol. 0.429 g (7.38 mmol) KF were added and the solution was degassed. Subsequently, 0.365 g (0.98 mmol) Cu(CH<sub>3</sub>CN)<sub>4</sub>PF<sub>6</sub>, 0.062 g (0.98 mmol) Cu(0) and 1.7 ml (9.84 mmol, 1.27 g) DIPEA were added, and stirring was continued at rt for 3 days. The mixture was then diluted with 100 ml DCM and 30 ml water/10 ml 25% ammonia. The layers were separated and the organic layer was washed with 30 ml 0.1 M disodium dihydrogen ethylenediaminetetraacetate (Na<sub>2</sub>-EDTA) solution/10 ml 25% ammonia. It was dried over Na<sub>2</sub>SO<sub>4</sub> and the solvent was removed *in vacuo*. Purification *via* column chromatography on basic alumina with PE/DCM 1 : 2, then 100% DCM as eluent, afforded 1.35 g (4.40 mmol, 89%) of the product as a white solid. <sup>1</sup>H-NMR (CDCl<sub>3</sub>, 400 MHz): δ = 0.88 (m, 3H, H-6''), 1.31 (m, 6H, H-3'', H-4'', H-5''), 1.64 (qui, 2H, <sup>3</sup>J = 7.7 Hz, H-2''), 2.67 (t, 2H, <sup>3</sup>J = 7.6 Hz, H-1''), 7.26 (m, 1H, H-5), 7.33 (d, 2H, <sup>3</sup>J = 8.4 Hz, H-3'), 7.70 (d, 2H, <sup>3</sup>J = 8.4 Hz, H-2'), 7.82 (td, 1H, <sup>3</sup>J = 7.8 Hz, <sup>4</sup>J = 1.7 Hz, H-4), 8.26 (dd, 1H, <sup>3</sup>J = 7.9 Hz, <sup>4</sup>J = 0.7 Hz, H-3), 8.59 (m, 1H, triazole-H), 8.62 (m, 1H, H-6). <sup>13</sup>C-NMR (CDCl<sub>3</sub>, 100 MHz): δ = 14.1 (C-6''), 22.6 (C-5''), 28.8, 31.3, 31.6 (C-4'', C-3'', C-2''), 35.5 (C-1''), 120.0 (C-5), 120.3 (C-3'), 120.5 (C-3), 123.0 (C=CH), 129.7 (C-2'), 134.7 (C-1'), 137.2 (C=CH), 144.0 (C-4), 148.5 (C-4'), 149.2 (C-6), 149.9 (C-2). MS (CI, 100 eV): *m/z* = 308 (22%), 307 (100%), 306 (7%), 279 (30%), 278

(40%), 207 (14%). *R<sub>F</sub>*-value: 0.33 (basic alumina, DCM/PE 1 : 1). Mp. 93 °C. IR (KBr): [cm<sup>-1</sup>] = 3129 (m), 1602 (s, C=N), 1520 (s). Elemental analysis (%): calc. C: 74.48, H: 7.24, N: 18.29; found C: 74.57, H: 7.24, N: 18.36.

#### 2-Azidopyridine (8)

1.23 ml (12.66 mmol, 2.0 g) 2-Bromopyridine was dissolved in 42 ml ethanol and 18 ml water and the solution was degassed. 1.65 g (25.32 mmol) Sodium azide, 0.24 g (1.27 mmol) CuI, 0.13 g (0.63 mmol) sodium ascorbate and 0.2 ml (1.90 mmol, 0.17 g) DMEDA were added. The suspension was heated under reflux for 1 h. After cooling to rt 100 ml water and 50 ml DCM were added. The layers were separated and the aqueous layer was extracted with 100 ml DCM. The combined organic layers were washed with 100 ml water and were dried over Na<sub>2</sub>SO<sub>4</sub>. The solvent was removed in vacuo and it was purified *via* column chromatography with basic alumina and DCM. 1.04 g (8.66 mmol, 68%) of a white solid was obtained. <sup>1</sup>H-NMR (CD<sub>3</sub>Cl, 400 MHz): δ = 7.24 (td, 1H, <sup>3</sup>J = 6.9 Hz, <sup>4</sup>J = 1.0 Hz, H-5), 7.68 (ddd, 1H, <sup>3</sup>J = 9.0 Hz, <sup>3</sup>J = 7.0 Hz, <sup>4</sup>J = 1.1 Hz, H-4), 8.05 (dt, 1H, <sup>3</sup>J = 9.0 Hz, <sup>4</sup>J = 1.1 Hz, H-3), 8.84 (dt, 1H, <sup>3</sup>J = 7.0 Hz, <sup>4</sup>J = 1.1 Hz, H-6). <sup>13</sup>C-NMR (CD<sub>3</sub>Cl, 100 MHz): δ = 116.0 (C-5), 116.2 (C-3), 125.4 (C-4), 131.8 (C-6), 148.6 (C-2). *R<sub>F</sub>*-value: 0.66 (basic alumina, DCM).

#### 2-(4-(4-Hexylphenyl)-1H-1,2,3-triazol-1-yl)pyridine (10)

136 mg (0.733 mmol) 1-Ethynyl-4-n-hexylbenzene and 88 mg (0.733 mmol) 2-azidopyridine **8** were dissolved in 40 ml DCM and 10 ml methanol and the solution was degassed. 55 mg (0.147 mmol) Cu(CH<sub>3</sub>CN)<sub>4</sub>PF<sub>6</sub>, 9 mg (0.147 mmol) Cu<sup>0</sup> and 0.25 ml (1.47 mmol, 0.189 g) DIPEA were added and it was heated under reflux for five days. After cooling to rt, 20 ml 25% ammonia in 80 ml water and 100 ml DCM were added. After stirring the solution vigorously for some minutes the layers were separated and the aqueous layer was extracted with 50 ml DCM. The combined organic layers were washed with 90 ml 0.1 M Na<sub>2</sub>-EDTA solution/10 ml 25% ammonia and dried over MgSO<sub>4</sub>. The solvent was removed in vacuo and it was purified *via* column chromatography on basic alumina and DCM and petrol ether 2 : 3 as eluent. 163 mg (0.532 mmol, 73%) Product was obtained as white crystals. <sup>1</sup>H-NMR (CD<sub>3</sub>Cl, 400 MHz): δ = 0.89 (m, 3H, H-6''), 1.32 (m, 6H, H-5'', H-4'', H-3''), 1.66 (qui, 2H, <sup>3</sup>J = 7.6 Hz, H-2''), 2.64 (t, 2H, <sup>3</sup>J = 7.7 Hz, H-1''), 7.28 (d, 2H, <sup>3</sup>J = 8.2 Hz, H-2'), 7.36 (ddd, 1H, <sup>3</sup>J = 6.5 Hz, <sup>3</sup>J = 4.9 Hz, <sup>4</sup>J = 0.9 Hz, H-4), 7.85 (d, 2H, <sup>3</sup>J = 8.2 Hz, H-3'), 7.94 (td, 1H, <sup>3</sup>J = 7.6 Hz, <sup>3</sup>J = 1.8 Hz, H-5), 8.26 (d, 1H, <sup>3</sup>J = 8.2 Hz, H-3), 8.53 (m, 1H, H-6), 8.78 (s, 1H, triazole-H). <sup>13</sup>C-NMR (CD<sub>3</sub>Cl, 100 MHz): δ = 14.1 (C-6''), 22.6 (C-5''), 29.0 (C-4''), 31.4 (C-3''), 31.7 (C-2''), 35.8 (C-1''), 113.8 (C=CH-triazole), 116.4 (C-5), 123.5 (C-4), 125.8 (C-2'), 127.6 (C-1'), 128.9 (C-3'), 139.1 (C-3), 143.4 (C-4'), 148.2 (C<sub>q</sub>-triazole), 148.5 (C-6), 149.2(C-2). CI-MS (100 eV): *m/z* = 307 (100%, M + H<sup>+</sup>), 279 (35%). *R<sub>F</sub>*-value: 0.19 (basic alumina, DCM/petrol ether 2 : 3). Mp. 60 °C. IR (KBr): [cm<sup>-1</sup>] = 3146 (m), 1611 (m), 1595 (s, C=N), 1577 (s), 1471 (s), 1461 (s). Elemental analysis (%): calc. C: 74.48, H: 7.24, N: 18.29; found C: 74.34, H: 7.22, N: 18.21.

### Ru(2-(1-(4-hexylphenyl)-1*H*-1,2,3-triazol-4-yl)pyridine)(2,2'-bipyridine-4,4'-dicarboxylic acid)(NCS)<sub>2</sub> TBA salt (1)

100 mg (0.326 mmol) Triazolyl-pyridine ligand **6** was dissolved in 50 ml dry DMF and the solution was degassed. 100 mg (0.163 mmol) [RuCl<sub>2</sub>(*p*-cymene)]<sub>2</sub> was added and the solution was heated with stirring to 75 °C in the dark for 6 h. Then, 80 mg (0.326 mmol) *dc bpy* was added and it was heated to 140 °C for 4 h. Subsequently, 1.0 g (excess) NH<sub>4</sub>NCS was added and it was heated to 145 °C for additional 4 h with constant stirring. It was cooled to rt overnight and then the solvent was removed *in vacuo* until about 5 ml of DMF remained. 50 ml water was added and the suspension was left in the ultrasonic bath for 30 min. It was cooled to 4 °C in the refrigerator overnight. The brown solid was filtered off and it was washed with large amounts of water and then diethyl ether. The crude material was dried *in vacuo*. The product was purified *via* column chromatography on Sephadex LH20, by dissolving the complex in methanolic tetra-*n*-butylammonium (TBA) hydroxide solution and methanol was used as eluent. The volume of the main fraction was reduced *in vacuo* and the brown product was precipitated with diethyl ether, collected by filtration and dried in high vacuum. <sup>1</sup>H NMR (d<sub>4</sub>-MeOH, 400 MHz): δ = 0.89 [0.95] (t, 3H, H-10'), 1.02 (t, 12H, TBA), 1.31 (m, 6H, H-7', H-8', H-9'), 1.43 (sext, 8H, TBA), 1.69 (m, 10H, TBA + H-6'), 2.65 [2.80] (t, 2H, H-5'), 3.26 (m, 8H, TBA), 7.11 [7.80] (td, 1H, H-5), 7.31 [7.47] (d, 2H, H-3'), 7.50 [7.53] (d, 2H, H-2'), 7.63 (dd, 1H, H-5''), 7.75 (td, 1H, H-4), 7.87 (d, 1H, H-5''), 7.99–8.17 (m, 2H, H-6, H-6''), 8.24 (m, 1H, H-6''), 8.83 [8.87] (s, 1H, H-3''), 8.95 [9.03] (s, 1H, H-3''), 9.33 [9.61] (s, 1H, triazole-H), 9.41 [9.57] (d, 1H, H-3). HR-MS (ESI): found *m/z* = 1008.36 (M + 1TBA - H<sup>+</sup>; C<sub>49</sub>H<sub>64</sub>N<sub>9</sub>O<sub>4</sub>RuS<sub>2</sub>); calc. *m/z* = 1008.36 for C<sub>49</sub>H<sub>64</sub>N<sub>9</sub>O<sub>4</sub>RuS<sub>2</sub>. IR (KBr): [cm<sup>-1</sup>] = 2107 (s, NCS). Elemental analysis (%) (C<sub>33</sub>H<sub>29</sub>N<sub>8</sub>O<sub>4</sub>RuS<sub>2</sub> • 1.3TBA • 3H<sub>2</sub>O): calc. C: 57.04, H: 7.31, N: 11.43; found C: 56.85, H: 7.22, N: 11.30.

### Ru(2-(4-(4-hexylphenyl)-1*H*-1,2,3-triazol-1-yl)pyridine)(2,2'-bipyridine-4,4'-dicarboxylic acid)(NCS)<sub>2</sub> TBA salt (2)

The complex was synthesized in an identical manner to complex **1** using 92 mg (0.30 mmol) triazolyl-pyridine ligand **10**, 92 mg (0.15 mmol) [RuCl<sub>2</sub>(*p*-cymene)]<sub>2</sub>, 73 mg (0.30 mmol) *dc bpy* ligand and 1.0 g (excess) NH<sub>4</sub>NCS. <sup>1</sup>H NMR (d<sub>4</sub>-MeOH, 400 MHz) δ = 0.87 [0.92] (t, 3H, H-10'), 1.01 (t, 12H, TBA), 1.29 (m, 6H, H-7', H-8', H-9'), 1.40 (sext, 8H, TBA), 1.58 (qui, 2H, H-6'), 1.66 (m, 8H, TBA), 2.58 [2.72] (t, 2H, H-5'), 3.23 (m, 8H, TBA), 7.18 [7.41] (d, 2H, H-3'), 7.26 [7.90] (t, 1H, H-5), 7.56 (d, 2H, H-2'), 7.61 (m, 1H, H-4), 7.62 (m, 1H, H-5''), 7.89 (m, 1H, H-5''), 8.09 [8.25] (d, 1H, H-6), 8.20 (m, 1H, H-6''), 8.34 (m, 1H, H-6''), 8.85 [8.87] (s, 1H, H-3''), 8.98 [9.03] (s, 1H, H-3''), 9.37 [9.50] (d, 1H, H-3), 9.49 [9.71] (s, 1H, triazole-H). HR-MS (ESI): *m/z* = 1008.36 (M + 1TBA - H<sup>+</sup>; C<sub>49</sub>H<sub>64</sub>N<sub>9</sub>O<sub>4</sub>RuS<sub>2</sub>); calc. *m/z* = 1008.36 for C<sub>49</sub>H<sub>64</sub>N<sub>9</sub>O<sub>4</sub>RuS<sub>2</sub>. IR (KBr): [cm<sup>-1</sup>] = 2107 (s, NCS). Elemental analysis (%) (C<sub>33</sub>H<sub>29</sub>N<sub>8</sub>O<sub>4</sub>RuS<sub>2</sub> • 1.3TBA • 3H<sub>2</sub>O): calc. C: 57.04, H: 7.31, N: 11.43; found C: 57.23, H: 7.62, N: 10.91.

### Device fabrication

Screen-printed layers of TiO<sub>2</sub> particles were employed as photoelectrodes in this study. An 8 μm thick transparent film of 20

nm sized TiO<sub>2</sub> particles was first printed on the fluorine doped SnO<sub>2</sub> (FTO) conducting glass electrode and subsequently coated with a 5 μm thick second layer of 400 nm light-scattering anatase particles (CCIC, Japan). The porosity was determined from BET measurements to be 68% for the 20 nm TiO<sub>2</sub> transparent layer and 42% for the 400 nm TiO<sub>2</sub> scattering layer. The detailed methods for TiO<sub>2</sub> film preparation, device fabrication, and the photocurrent-voltage measurements can be found in an earlier report.<sup>16</sup> After sintering at 500 °C and cooling to 80 °C, the sintered TiO<sub>2</sub> electrodes were sensitized by dipping 16 h into the dye solution (300 μM) in 10% DMSO and acetonitrile and *tert*-butyl alcohol (volume ratio 1 : 1) mixture, with 75 μM DINHOP (4 : 1) as a co-adsorbent. For the solid-state devices, a compact TiO<sub>2</sub> layer was first deposited onto the FTO substrate by spray pyrolysis, onto which 23 nm sized TiO<sub>2</sub> particles were deposited by doctor-blading to obtain a 2 μm thick mesoporous film. After sintering the TiO<sub>2</sub> layers at 500 °C, the film was cooled to room temperature and immersed overnight in 0.02 M aqueous TiCl<sub>4</sub>. The film was then rinsed with deionized water, annealed in air at 450 °C for 20 min, and cooled to 80 °C before immersing it in the dye solution (300 μM) for sensitization. The hole transporting material solution containing 0.17 M spiro-MeOTAD, 0.11 mM *tert*-butylpyridine, and 0.21 mM LiN(CF<sub>3</sub>SO<sub>2</sub>)<sub>2</sub> in chlorobenzene was used. We deposited this solution onto the dye-coated TiO<sub>2</sub> film, leaving it to penetrate into the pores of the TiO<sub>2</sub> layer for 1 min prior to spin-coating. Finally, a 50 nm-thick gold contact was deposited onto the organic semiconductor to close the cell.

### Transient absorption spectroscopy

The photovoltage transient decay was recorded using an exciting pulse generated by a ring of red LEDs (Lumiled) controlled by a fast solid-state switch. The pulse widths were 100 ms. The pulse was incident on the photoanode side of the device. An array of InGaN diodes (Lumiled) supplied the white bias light incident from the same direction. Transients were measured at different white light intensities *via* tuning the voltage applied to the bias diodes. Before the LEDs switched to the next light intensity, a charge-extraction routine was executed to measure the electron density in the film. In the charge-extraction technique, the LED illumination source was turned off in <1 μs, while the cell was simultaneously switched from open to short circuit. The resulting current, as the cell returned to *V* = 0 and *J* = 0, was integrated to give a direct measurement of the excess charge in the film at that *V*<sub>OC</sub>.

### Acknowledgements

The authors thank the German Ministry of Education and Research (BMBF) in the frame of project OPEG 2010 and the Swiss National Science Foundation for the financial support.

### References

- 1 B. O'Regan and M. Grätzel, *Nature*, 1991, **353**, 737.
- 2 Reviews: (a) M. Grätzel, *Nature*, 2001, **414**, 338; (b) A. Hagfeldt and M. Grätzel, *Acc. Chem. Res.*, 2000, **33**, 269; (c) M. Grätzel, *Acc. Chem. Res.*, 2009, **42**, 1788.
- 3 (a) M. K. Nazeeruddin, A. Kay, L. Rodicio, R. Humphry-Baker, E. Müller, P. Liska, N. Vlachopoulos and M. Grätzel, *J. Am.*

- Chem. Soc.*, 1993, **115**, 6382; (b) Md. K. Nazeeruddin, P. Péchy and M. Grätzel, *Chem. Commun.*, 1997, 1705; (c) P. Wang, B. Wenger, R. Humphry-Baker, J. E. Moser, J. Teuscher, W. Kantelechner, J. Mezger, E. V. Stoyanov, S. M. Zakeeruddin and M. Grätzel, *J. Am. Chem. Soc.*, 2005, **127**, 6850; (d) Md. K. Nazeeruddin, F. De Angelis, S. Fantacci, A. Selloni, G. Viscardi, P. Liska and M. Grätzel, *J. Am. Chem. Soc.*, 2005, **127**, 16835; (e) P. Wang, C. Klein, R. Humphry-Baker, S. M. Zakeeruddin and M. Grätzel, *Appl. Phys. Lett.*, 2005, **86**, 123508; (f) Y. Bai, Y. Cao, J. Zhang, M. Wang, R. Li, P. Wang, S. M. Zakeeruddin and M. Grätzel, *Nat. Mater.*, 2008, **7**, 626; (g) F. Gao, Y. Cheng, Q. Yu, S. Liu, D. Shi, Y. Li and P. Wang, *Inorg. Chem.*, 2009, **48**, 2664; (h) A. Mishra, N. Pootrakulchote, M. K. R. Fischer, C. Klein, M. K. Nazeeruddin, S. M. Zakeeruddin, P. Bäuerle and M. Grätzel, *Chem. Commun.*, 2009, 7146; (i) J.-P. Sauvage, M. K. R. Fischer, A. Mishra, S. M. Zakeeruddin, M. K. Nazeeruddin, P. Bäuerle and M. Grätzel, *ChemSusChem*, 2009, **2**, 761; (j) C.-Y. Chen, M. Wang, J.-Y. Li, N. Pootrakulchote, L. Alibabaei, C.-h. Ngoc-le, J.-D. Decoppet, J.-H. Tsai, C. Grätzel, C.-G. Wu, S. M. Zakeeruddin and M. Grätzel, *ACS Nano*, 2009, **3**, 3103.
- 4 (a) A. S. Polo, M. K. Itokazu and N. Y. M. Iha, *Coord. Chem. Rev.*, 2004, **248**, 1343; (b) H. Hofmeier and U. S. Schubert, *Chem. Soc. Rev.*, 2004, **33**, 373; (c) C. Kaes, A. Katz and M. W. Hosseini, *Chem. Rev.*, 2000, **100**, 3553.
- 5 (a) R. Hage, J. G. Haasnoot, J. Reedijk, R. Wang and G. J. Vos, *Inorg. Chem.*, 1991, **30**(17), 3263; (b) A. C. Lees, B. Evrard, T. E. Keyes, J. G. Vos, C. J. Kleverlaan, M. Alebbi and C. A. Bignozzi, *Eur. J. Inorg. Chem.*, 1999, **12**, 2309; (c) S. Fanni, T. E. Keyes, C. M. O'Connor, H. Hughes, R. Wang and J. G. Vos, *Coord. Chem. Rev.*, 2000, **208**, 77; (d) B. Pradhan and S. Das, *Chem. Mater.*, 2008, **20**(4), 1209.
- 6 (a) H. C. Kolb, M. G. Finn and K. B. Sharpless, *Angew. Chem., Int. Ed.*, 2001, **40**, 2004; (b) C. W. Tornøe, C. Christensen and M. Meldal, *J. Org. Chem.*, 2002, **67**, 3057; (c) A. D. Bock, H. Hiemstra and J. H. van Maarseveen, *Eur. J. Org. Chem.*, 2006, 51; (d) J.-F. Lutz, *Angew. Chem., Int. Ed.*, 2007, **46**, 1018; (e) R. M. Meudtner, M. Ostermeier, R. Goddard, C. Limberg and S. Hecht, *Chem.–Eur. J.*, 2007, **13**, 9834.
- 7 (a) C. Richardson, C. M. Fitchett, F. R. Keene and P. J. Steel, *Dalton Trans.*, 2008, 2534; (b) Y. Li, J. C. Huffman and A. H. Flood, *Chem. Commun.*, 2007, 2692; (c) C. M. Fitchett, F. R. Keene, C. Richardson and P. J. Steel, *Inorg. Chem. Commun.*, 2008, **11**, 595; (d) J. T. Fletcher, B. J. Bumgarner, N. D. Engels and D. A. Skoglund, *Organomet.*, 2008, **27**, 5430; (e) U. Monkowius, S. Ritter, B. König, M. Zabel and H. Yersin, *Eur. J. Inorg. Chem.*, 2007, 4597.
- 8 (a) B. Happ, C. Friebe, A. Winter, M. D. Hager, R. Hoogenboom and U. S. Schubert, *Chem.–Asian J.*, 2009, **4**, 154; (b) B. Happ, D. Escudero, M. D. Hager, C. Friebe, A. Winter, H. Görls, E. Altuntas, L. González and U. S. Schubert, *J. Org. Chem.*, 2010, **75**, 4025; (c) B. Schulze, C. Friebe, M. D. Hager, A. Winter, R. Hoogenboom, H. Görls and U. S. Schubert, *Dalton Trans.*, 2009, 787.
- 9 (a) K.-S. Chen, W.-H. Liu, Y.-H. Wang, C.-H. Lai, P.-T. Chou, G.-H. Lee, K. Chen, H.-Y. Chen, Y. Chi and F.-C. Tung, *Adv. Funct. Mater.*, 2007, **17**, 2964; (b) K.-L. Wu, H.-C. Hsu, K. Chen, Y. Chi, M.-W. Chung, W.-H. Liu and P.-T. Chou, *Chem. Commun.*, 2010, **46**, 5124.
- 10 S. Paek, C. Baik, M.-S. Kang, H. Kang and J. Ko, *J. Organomet. Chem.*, 2010, **695**, 821.
- 11 J. Andersen, U. Madsen, F. Björkling and X. Liang, *Synlett*, 2005, 2209.
- 12 T. Johansson, W. Mammo, M. Svensson, M. R. Andersson and O. Inganäs, *J. Mater. Chem.*, 2003, **13**, 1316.
- 13 B. O'Regan, K. Walley, M. Juozapavicius, A. Anderson, F. Matar, T. Ghaddar, S. M. Zakeeruddin, C. Klein and J. Durrant, *J. Am. Chem. Soc.*, 2009, **131**, 3541.
- 14 (a) S. Huang, G. Schlichthörl, A. Noyik, M. Grätzel and A. Frank, *J. Phys. Chem. B*, 1997, **101**, 2576; (b) B. O'Regan and J. R. Durrant, *Acc. Chem. Res.*, 2009, **42**, 1799.
- 15 B. T. Holmes, W. T. Pennington and T. W. Hanks, *Synth. Commun.*, 2003, **33**, 2447.
- 16 P. Wang, S. M. Zakeeruddin, P. Comte, R. Charvet, R. Humphry-Baker and M. Graetzel, *J. Phys. Chem. B*, 2003, **107**, 14336.